



# Robust RBM3 and $\beta$ -klotho expression in developing neurons in the human brain

Travis C Jackson<sup>1</sup>, Keri Janesko-Feldman<sup>2,3</sup>, Shaun W Carlson<sup>4</sup>, Shawn E Kotermanski<sup>5</sup> and Patrick M Kochanek<sup>2,3</sup>

## Abstract

RNA binding motif 3 (RBM3) is a powerful neuroprotectant that inhibits neurodegenerative cell death in vivo and is a promising therapeutic target in brain ischemia. RBM3 is increased by the hormone fibroblast growth factor 21 (FGF21) in an age- and temperature-dependent manner in rat cortical neurons. FGF21 receptor binding is controlled by the transmembrane protein  $\beta$ -klotho, which is mostly absent in the adult brain. We discovered that RBM3/ $\beta$ -klotho is unexpectedly high in the human infant vs. adult brain (hippocampus/prefrontal cortex). The use of tissue homogenates in that study precluded a comparison of RBM3/ $\beta$ -klotho expression among different CNS cell-types, thus, omitted key evidence (i.e. confirmation of neuronal expression) that would otherwise provide a critical link to support their possible direct neuroprotective effects in humans. This report addresses that knowledge gap. High-quality fixed human hippocampus, cortex, and hypothalamic tissues were acquired from the NIH Neurobiobank (<1 yr (premature born) infants, 1 yr, 4 yr, and 34 yr). Dual labeling of cell-type markers vs. RBM3/ $\beta$ -klotho revealed enriched staining of targets in neurons in the developing brain. Identifying that RBM3/ $\beta$ -klotho is abundant in neurons in the immature brain is fundamentally important to guide protocol design and conceptual frameworks germane to future testing of these neuroprotective pathways in humans.

## Keywords

RNA binding motif 3, klotho, fibroblast growth factor 21, cortex, development

Received 12 April 2019; Revised 3 September 2019; Accepted 4 September 2019

## Introduction

RNA binding motif 3 (RBM3) is a neuroprotective cold-shock protein (CSP), and improves neurological function in transgenic mice with severe neurodegenerative disease.<sup>1–3</sup> The intracellular mechanisms mediating RBM3 neuroprotection remain to be fully elucidated. In part, its benefits are thought to involve: increased rates of global protein synthesis, modulation of miRNA maturation, increased expression of reticulon-3, and inhibition of caspases, among other mechanisms.<sup>1,4–7</sup> Its potent cerebroprotective effects in pre-clinical models of brain injury have prompted a surge in clinical interest on RBM3 and other CSPs, and increased efforts to identify pharmacological approaches to either augment their induction at normothermia in the treatment of either acute and chronic brain injury, or to enhance the efficacy of neuroprotective therapeutic hypothermia in neuro critically ill patients.<sup>4</sup> The robustness of RBM3-dependent

neuroprotection in rodents underscores the need for additional research to better characterize RBM3 biology in the human brain, and to determine if characteristics of its homeostatic regulation are shared across species.

<sup>1</sup>Department of Molecular Pharmacology & Physiology, Morsani College of Medicine, University of South Florida, Tampa, FL, USA

<sup>2</sup>Safar Center for Resuscitation Research, School of Medicine Children's Hospital of Pittsburgh of UPMC John G. Rangos Research Center, University of Pittsburgh, Pittsburgh, PA, USA

<sup>3</sup>Department of Critical Care Medicine, School of Medicine, University of Pittsburgh, Pittsburgh, PA, USA

<sup>4</sup>Department of Neurological Surgery, School of Medicine, University of Pittsburgh, Pittsburgh, PA, USA

<sup>5</sup>Department of Pharmacology and Chemical Biology, School of Medicine, University of Pittsburgh, Pittsburgh, PA, USA

## Corresponding author:

Travis C Jackson, Department of Molecular Pharmacology & Physiology, Morsani College of Medicine, University of South Florida, 12901 Bruce B Downs BLDV, MDC 2532, Tampa, FL 33612-4799, USA.  
Email: tcjacksontc@health.usf.edu

Several important features of RBM3 biology brought to light in rodents are conceptually important, and their conservation or variation across species may influence the extent that CSPs are similarly neuroprotective in humans and/or help to define the clinical settings in which their manipulation may be most beneficial.<sup>4</sup> First, newborn rats and mice have increased baseline RBM3 levels at normothermia, whereas levels are low/absent at baseline in the adult rodent brain.<sup>1,8</sup> Thus, RBM3 signaling may have a substantially greater capacity to be manipulated in newborns. Importantly, recent work confirmed that RBM3 is also developmentally regulated in the human brain (hippocampus and prefrontal cortex (PFC)), and showed that maximal protein expression is seen during infancy whereas levels are low/absent in adults.<sup>9</sup> A second important homeostatic characteristic of RBM3 brought to light via histological studies in newborn rodents was the observation that at normothermia it is mainly found in neurons with very little expression in glia such as astrocytes. Furthermore, at the subcellular level, RBM3 localized mostly in the nucleus during early CNS development.<sup>8</sup> Thus, the abundance of RBM3 specifically in neurons is key evidence that supports its presumed direct neuroprotective effects in rodent pre-clinical models of brain injury. A major gap in understanding is whether or not RBM3 is also present in human neurons, and if neurodevelopmental age alters its neuronal targeting as it does in rodents. Here we provide a multi-age histological examination of baseline neuronal RBM3 in the human brain to provide additional clarity germane to the optimal developmental time window(s) for targeting RBM3 neuroprotective mechanisms with future therapies.

Chemical and/or biological agents able to augment the induction of RBM3 during cooling or at normothermia have considerable clinical interest. The endocrine hormone fibroblast growth factor 21 (FGF21) readily crosses the blood–brain barrier, is a novel neuroprotectant, and is increased systemically in the circulation by cold stress.<sup>10–14</sup> Administration of exogenous FGF21 *in vitro* augmented RBM3 levels in immature primary rat cortical neurons after 24 h of ultra-mild hypothermia—with as little as a single degree centigrade of temperature reduction.<sup>15</sup> Circulating FGF21 activates downstream signaling mechanisms only in cells which express the transmembrane co-receptor protein  $\beta$ -klotho, which is restricted to a few sites in the body.<sup>16,17</sup> In the adult brain,  $\beta$ -klotho is primarily found in the hypothalamus, hind-brain, and nucleus accumbens, based on studies in mice.<sup>18,19</sup> In contrast, it was recently reported that  $\beta$ -klotho is surprisingly abundant in the hippocampus and in the PFC in the human infant brain but expectedly absent in these regions in the adult brain.<sup>9</sup>

However, a topographical analysis was not performed and thus, it remains unclear which cell type(s) represent the primary source of  $\beta$ -klotho in the infant human brain. Here we report robust expression of RBM3 and  $\beta$ -klotho in neurons of the hippocampus and PFC in the infant human brain.

## Materials and methods

### Chemicals and reagents

Antibodies: Monoclonal anti-glial fibrillary acidic protein (GFAP), Cat# ab10062, Lot# GR3203491-6; monoclonal anti-neuronal nuclei (NeuN), Cat# ab104224, Lot# GR3227256-2; polyclonal anti- $\beta$ -klotho, Cat# ab106794, Lot# GR3242063-1 (Abcam; Cambridge, MA). Polyclonal Anti-RBM3, Cat# 14363-1-AP, Lot# 00039939 (Proteintech, Chicago, IL). Polyvinylidene fluoride or polyvinylidene difluoride (PVDF) membrane: The mdi brand PVDF was used to detect RBM3 and  $\beta$ -klotho (MDI Membrane Technologies, Harrisburg, PA), 0.2  $\mu$ M pore-size, Cat# SVFX8301XXXX101, Lot# VA760606L.

### NIH NeuroBioBank (NBB) human brain specimens

Formalin fixed brain tissues: Specimens used for immunohistochemistry (IHC) analysis were pre-selected by study investigators based on subject age, diagnosis (“unaffected control”), and tissue availability. Two different male subjects (S1 and S2) were requested for each age and included: <1-year-old premature infants born at 36 weeks (ID Code #5817 and #4428), 1 year-old (ID Code #1488 and #1547), 4 year-old (ID Code #451 and #4218), and 34 year-old (ID Code #5648 and #5759). The exact subject age in order is: 213 days (#5817), 142 days (#4428), 1 year + 138 days (#1488), 1 year + 260 days (#1547), 4 years + 204 days (#451), 4 years + 169 days (#4218), 34 years + 343 days (#5648), and 34 years + 136 days (#5759). Fixed human brain specimens were obtained from the NBB after approval by NIH staff, and supplied in sealed plastics bags that contained storage buffer. Human brain tissue homogenates: whole extract hippocampal and PFC homogenates were derived from two male infants (ID Code: #4411 and #4428) and two male adults (ID Code: #5614 and #5705). The preparation of human brain homogenates including protein concentration analysis from these tissues (i.e. prepared from frozen brain obtained from the NBB) was previously described.<sup>9</sup>

### Immunohistochemistry

An 8-mm biopsy puncher (Fisher Scientific, Pittsburgh, PA) was employed to extract equivalent sized pieces of

tissue from the center field of each brain region. Round-cut tissues were placed in cassettes for dehydration, and included six specimens per cassette (i.e. a piece of hippocampus, PFC, and hypothalamus from each of two patients of the same age). Tissues were taken through graded alcohols (70–100%), cleared with xylene, and embedded in Histoplast paraffin (Fisher Scientific). The process was repeated for all age groups (i.e. a total of four separate paraffin embedded (PE) blocks were made which encompassed 24 circular tissue specimens across all age groups and brain regions). PE tissue blocks were cut (5  $\mu$ M sections) on a microtome (Lieca; Buffalo Grove, IL). HistoBond Plus Super Mega slides (Ted Pella; Redding, CA) were used to combine (on a single slide) 5  $\mu$ M sections from all four age/PE-blocks. In this manner, IHC staining levels across all ages/brain regions could be appropriately compared by ensuring that treatment conditions were equivalent on all tissues. Tissues on slides were deparaffinized with xylene, rehydrated in graded alcohols, and washed with Tris-buffered saline (TBS) Auto Wash Buffer (BioCare Medical, Pacheco, CA). Tissue sections were submerged in Antigen Decloaker solution (BioCare Medical), and subsequently heated in a microwave for 10 min. The process was repeated twice for antigen retrieval. Slides were cooled for 20 min and washed twice (5 min each) in buffer. Endogenous peroxidase was inhibited using 0.03% H<sub>2</sub>O<sub>2</sub> in methanol for 30 min and sections were washed twice (5 min each) in buffer. All antibodies were used at 1:200 dilution. Hematoxylin counter staining was performed as described by our group.<sup>20</sup> Photomicrographs were collected on a Nikon Eclipse 90i using NIS ELEMENTS software at 10 $\times$  magnification (Nikon, Melville, NY). Quantification of  $\beta$ -klotho and RBM3 (DAB) in hematoxylin counter-stained sections was done using the Fiji Software processing package. In brief, representative images (unmodified 10 $\times$  magnification) of brain sections were first deconvoluted in Image J. Isolated color 3 (DAB) images were saved as 8-bit TIFF files. The signal-to-background threshold was adjusted in equal measure across all images (0–80). Total field optical density (OD) of grey pixels was measured and recorded for each image (mean and standard deviation). Data from two subjects were combined for a composite value of mean  $\pm$  SD.

For dual-labeling experiments, we used the ImmPRESS<sup>®</sup> Duet Double Staining kit (Vector Laboratories, Burlingame, CA). Tissue staining followed vendor-provided instructions. In brief, after an overnight incubation with the primary antibody, tissues were washed twice (10 min each) in buffer and slides were incubated for 10 min in ImmPRESS Duet Detection Reagent. Wash steps were repeated (5 min each) and slides were incubated for 2 min in

ImmPACT DAB EqV substrate to detect targets (RBM3 or  $\beta$ -klotho). Wash steps were repeated (5 min each) and slides were incubated for 2 min in ImmPACT Vector Red substrate to detect cell-type specific markers (NeuN or GFAP). Wash steps were repeated (5 min each) followed by a 5-min rinse in deionized water. Slides were dehydrated, cleared with xylene, and coverslips applied with Permount (Fisher Scientific). Photomicrographs were collected on a Nikon Eclipse 90i using NIS ELEMENTS software at 20 $\times$  magnification. The equivalent polyclonal anti-RBM3 and anti- $\beta$ -klotho antibodies used in a recent Western blot analysis of 78 high-quality human brain tissues were also used here for IHC.<sup>9</sup> However, the antibody lot numbers differed vs. prior work; therefore, we first confirmed the specificity of antibodies to detect study targets. Also, in pilot experiments, we explored the utility of immunofluorescent techniques to colocalize RBM3 with cell-type specific markers. However, substantial background auto-fluorescence precluded fluorescent microscopy of human brain specimens. These tissues, from the NIH sample repository, were harvested in a rigorously protocolized manner to generate high-quality specimens but storage in fixatives for months-years likely exacerbated auto-fluorescence. Alternatively, we used a dual chromogenic labeling approach to investigate cell-type specificity. The ImmPRESS<sup>®</sup> Duet Double Staining kit was employed to evaluate RBM3 or  $\beta$ -klotho (brown staining) against cell-type specific markers including GFAP vs. NeuN (red staining).

### Western blot

Protein analysis was performed as previously described by our group. In brief, 20  $\mu$ g/well brain extract was mixed with 2 $\times$  Laemmli buffer, and loaded onto 15-well precast sodium dodecyl sulfate (SDS) gradient TGX gels (BioRad, Hercules, CA). Kaleidoscope (colored) protein standards were included for molecular weight reference (BioRad). Gels were run at 150 V, and proteins were transferred to PVDF membranes by a  $\sim$ 1 h transfer at 100 V (4 $^{\circ}$ C) in buffer. Notably, we reported that a discontinued brand of PVDF membrane (0.45- $\mu$ M-pore-size Hybond-P, Cat#RPN2020F) had superior RBM3 detecting properties vs. numerous alternative PVDF brands.<sup>15</sup> Here we tested the commercially available mdi brand of PVDF membrane and found that it had similar performance to detect RBM3 (MDI Membrane Technologies) vs. the discontinued membrane. Thus, in our experience the mdi membrane is an excellent replacement product for RBM3 Western blot investigations. Following protein transfer, the Reversible Swift Membrane Stain (Fisher Scientific) was used to measure total protein

(i.e. loading control) as previously reported.<sup>9</sup> Membranes were blocked for 1h in 7.5% milk dissolved in TBS/tween-20 (TBST). Primary antibodies (1:1000) were applied overnight at 4°C on a rocker. Membranes were washed with TBS (3×/5min each), incubated for ~2h with secondary antibodies (1:15,000), washed in TBS (3×/5min each), incubated for 2min in ECL-2 Western blotting substrate (Fisher Scientific), membranes placed inside a plastic holder, blots exposed to film inside a cassette, and developed in a darkroom. Films were scanned on a 600 dpi flatbed scanner and images were compiled in Photoshop (Adobe, San Jose, CA).

## Results

The anti-RBM3 antibody recognized a single major band at ~17kDa in human male hippocampus and

PFC homogenates, which is the predicted molecular weight of RBM3 (Figure 1(a) and (b)). Moreover, RBM3 was abundant in the infant brain and comparatively absent/low in adults as expected. Interestingly, RBM3 levels were notably greater in the PFC vs. hippocampus at both ages (Figure 1(a)). The anti-β-klotho antibody showed similar findings. A single ~120kDa band as is its predicted molecular weight was detected in brain homogenates in infants and absent in adults (Figure 1(c) and (d)). Together, these results support the notion that both antibodies have high specificity, as assessed by SDS-polyacrylamide gel electrophoresis and demonstrate little or no cross-reactivity to non-specific targets in human brain tissue homogenates. Equal protein loading was confirmed by total protein stain (Figure 1(b) and (d), and Supplementary Figure 1).

Next, we performed RBM3/hematoxylin counter staining in brain tissue sections from male subjects

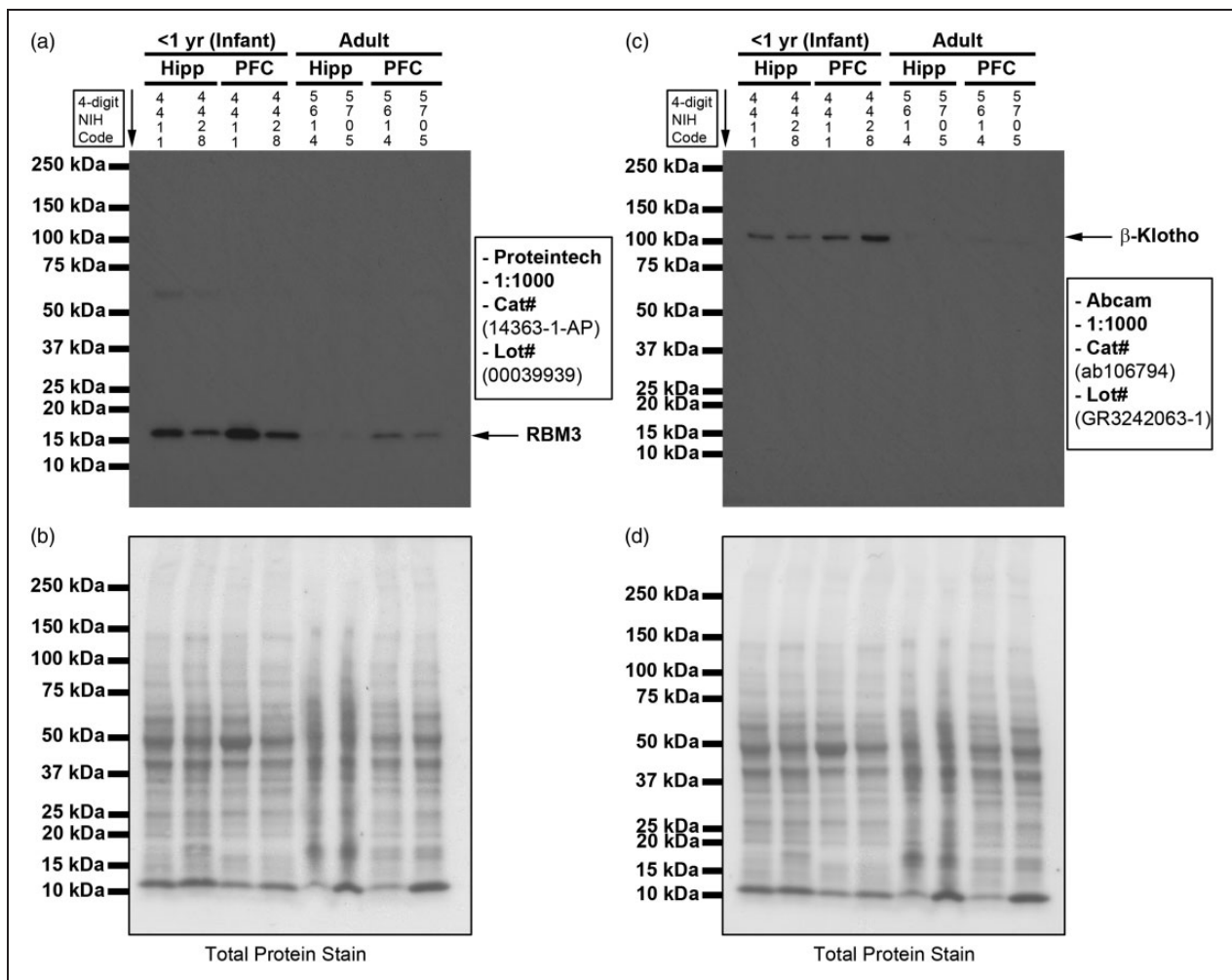


**Figure 1.** Validation of antibody specificity in human brain tissue homogenates. (a and c) Western blots show RBM3/β-klotho levels in the hippocampus and in the prefrontal cortex in infants ( $n=2$ ) and adults ( $n=2$ ). (b, d) Total protein stain shows equal loading and transfer across samples in RBM3/β-klotho Western blots. A single band is detected at ~17kDa for RBM3, and ~120kDa for β-klotho.

aged <1, 1, 4, and 34 years. RBM3 staining intensity was greatest in the hippocampus and in the PFC in <1 year infants (OD:  $9.11 \pm 4.52$  and  $11.95 \pm 1.34$ , respectively) and in 1 year-olds (OD:  $8.62 \pm 11.19$  and

$9.46 \pm 2.51$ , respectively). Furthermore, staining appeared concentrated in neurons, and at young ages in axonal projections (Figure 2 and Supplementary Table 1). RBM3 staining was sparse in the

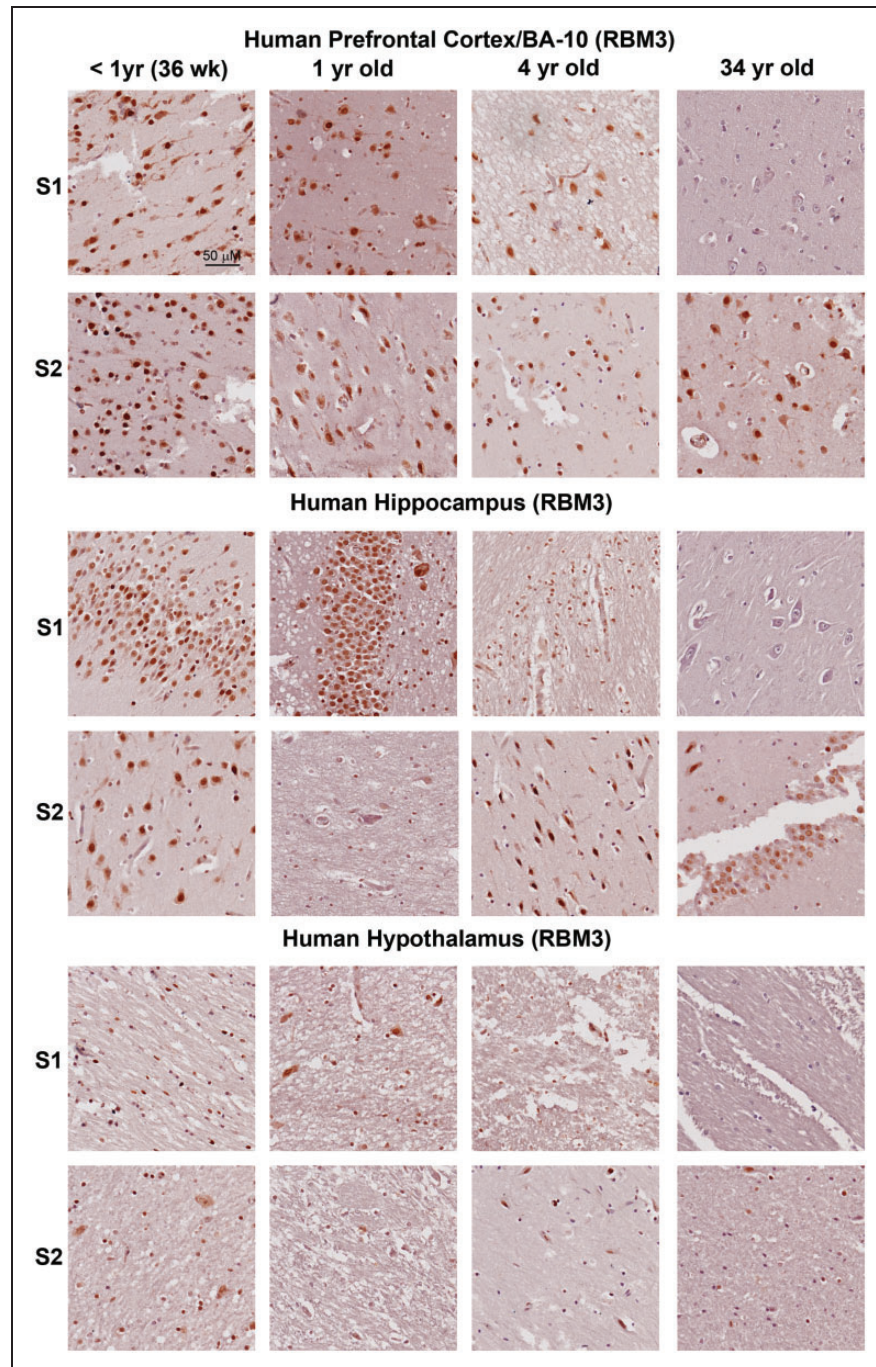


**Figure 2.** Comparison of RBM3/hematoxylin counter staining across all ages (infant-to-adult). Images (10× magnification) show representative staining levels of RBM3 (brown) for each age/brain region. Two different subjects within each age group are shown (S1 and S2). Relevant to the different brain regions, RBM3 staining intensity is greatest in the PFC > hippocampus > hypothalamus. Relevant to different ages, staining intensity is greatest in <1/1 year-old vs. 4/34 year-old. In infants, RBM3 is visible in axonal projections from PFC neurons.

hypothalamus but comparatively increased in the <1 year infants (OD:  $3.25 \pm 1.29$ , infants vs.  $1.94 \pm 2.12$ , 1 yr-old;  $1.08 \pm 0.34$ , 4 yr-old; and  $0.48 \pm 0.63$ , adult).

Next we co-labeled RBM3 with NeuN vs. GFAP. Signal separation manifests as two clearly distinguishable colors and indicates that the targets do not co-localize, whereas co-localization results in a single color. Tissues from 1 year-olds were chosen for dual-labeling experiments because they had the most intense RBM3 and  $\beta$ -klotho staining on initial IHC assessment. Anti-GFAP vs. anti-RBM3 staining showed distinct color separation (Figure 3). Hippocampal neurons within the stratum pyramidale revealed dark brown nuclei (RBM3) with discrete interspersed astrocyte projections (bright red). RBM3 was also visible in the neuronal cytoplasm but less intense vs. nuclear staining. Tissue staining with anti-NeuN vs. anti-RBM3 resulted in a single dark maroon color with no red/brown separation (Figure 4). These findings support the notion that, like rodents, RBM3 is abundant in neurons at baseline in the infant human brain.

Next, we performed  $\beta$ -klotho/hematoxylin counter staining in brain tissue sections from male subjects aged <1, 1, 4, and 34 years.  $\beta$ -klotho staining intensity

was greatest in the hippocampus and in the PFC in one year-olds (OD:  $34.89 \pm 38.48$  and  $85.01 \pm 56.71$ , respectively), and low in adults (OD:  $7.26 \pm 1.07$  and  $8.65 \pm 0.70$ , respectively). Furthermore,  $\beta$ -klotho staining was concentrated in neurons in the hippocampus (Figure 5 and Supplementary Table 2). Anti-GFAP vs. anti- $\beta$ -klotho staining showed distinct color separation in tissue sections from one year-olds (Figure 6). Furthermore, staining was robust in the membrane/cytoplasm and comparatively low in NeuN. Tissue staining with anti-NeuN vs. anti- $\beta$ -klotho resulted in a single deep maroon color (Figure 7). Notably, because NeuN primarily detected NeuN /soma, and  $\beta$ -klotho is enriched in the membrane/cytoplasm, nuclear red staining was readily distinguishable from the surrounding maroon color in a few neurons (e.g. the enlarged image of a hypothalamic neuron in S2, Figure 7).

## Discussion

Here we used IHC to determine if RBM3/ $\beta$ -klotho was expressed in neurons in the human brain. We confirm that humans share a second major trait germane to

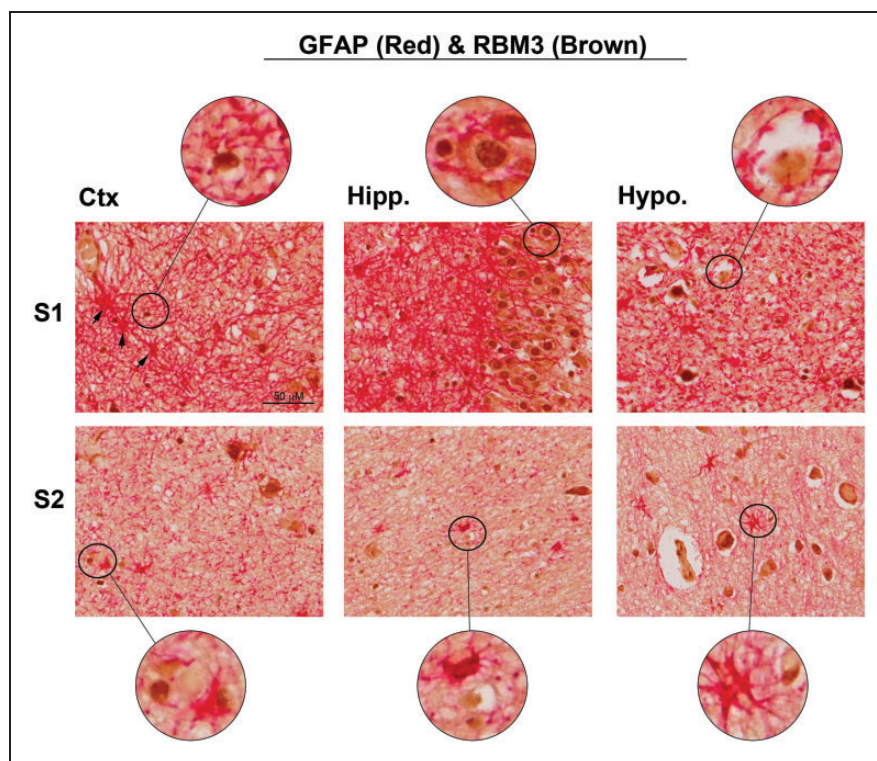


**Figure 3.** RBM3 and GFAP double-labeling in one-year-old tissue sections. Images (20 $\times$  magnification) show representative distribution of RBM3 (brown) and GFAP (red). RBM3 vs. GFAP staining does not co-localize. Circles show an enlarged view of typical staining patterns within each field. RBM3 (brown) intensity is greatest in the cell nucleus but is also visible in the cytoplasm of hippocampal neurons. Black arrows show a row of bright-red labeled astrocytes.

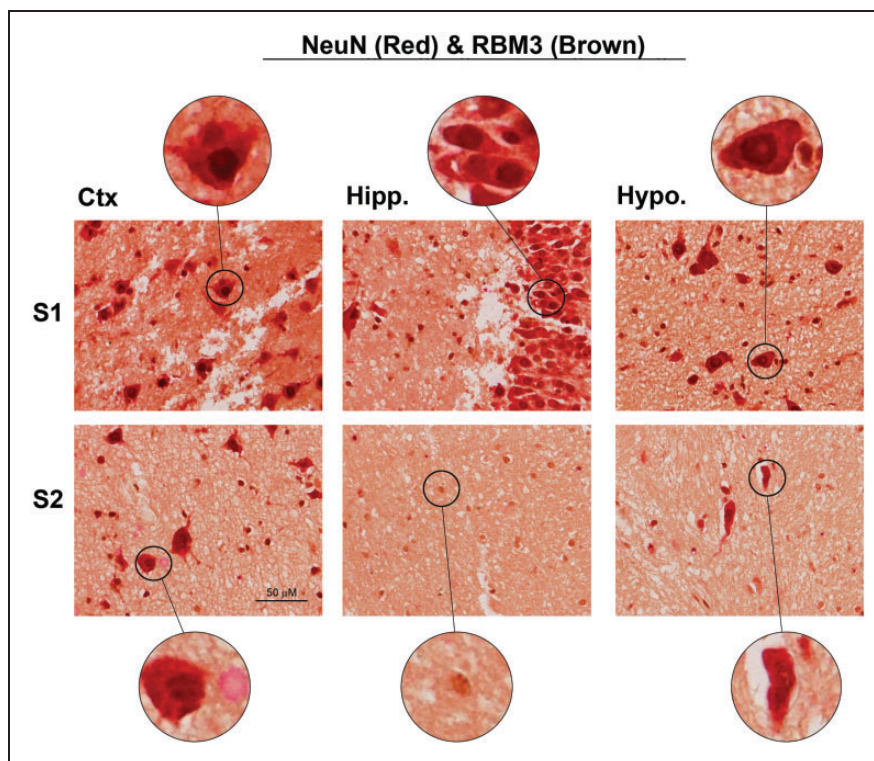


**Figure 4.** RBM3 and NeuN double-labeling in one-year-old tissue sections. Images (20 $\times$  magnification) show representative distribution of RBM3 (brown) and NeuN (red). RBM3 vs. NeuN staining results in a deep maroon color across all three brain regions, and is indicative of co-localization of brown/red labeling. Circles show an enlarged view of typical cell staining patterns within each field. Neuronal nuclei appear black in the PFC due to the increased intensity of RBM3 staining (dark brown) at that locus, and in combination with NeuN (red) which also preferentially stains neuronal nuclei.

RBM3 biology that has been observed in rodents,<sup>8</sup> namely, RBM3 is expressed and concentrated in human neurons. Moreover, in all brain regions examined, RBM3 staining was highest in infants (cortex,  $11.95 \pm 1.34$ ; hippocampus,  $9.11 \pm 4.52$ ; hypothalamus,  $3.25 \pm 1.29$ ) and lowest in adults (cortex,  $4.81 \pm 6.75$ ; hippocampus,  $1.93 \pm 2.71$ ; hypothalamus,  $0.48 \pm 0.63$ ). RBM3 is a potent neuroprotective CSP, and its induction decreases neuronal death *in vitro* and *in vivo*.<sup>1–3</sup> The results presented here strengthen the notion that novel strategies to augment RBM3 in pre-clinical models of brain injury merit additional study and may hold therapeutic promise for enhancing the survival and/or function of injured neurons in the human brain. While the results support the conclusion that RBM3 is abundant in neurons at baseline, our findings do not imply that therapies (e.g. cold-stress) selectively induce RBM3 in neurons. Indeed, RBM3 levels are also increased in rat astrocytes *in vitro* by exposing them to 33°C for 48 h.<sup>15</sup> Thus, cooling and/or other pharmacological strategies that increase RBM3 in the CNS may robustly target non-neuronal cells in the human brain as well.<sup>21,22</sup>

FGF21 is an endocrine hormone that promotes non-shivering thermogenesis in rodents and in humans, and is increased in blood plasma in response to, among

other stressors, environmental cold-stress.<sup>13,14</sup> FGF21 readily crosses the blood–brain barrier and it also regulates the circadian rhythm, alcohol intake, and sugar intake by stimulating  $\beta$ -klotho expressing neurons in the hypothalamus/nucleus accumbens.<sup>18,19,23</sup> Treatment of cultured rat cortical neurons with rFGF21 augmented hypothermic induction of RBM3 in immature day *in vitro* (DIV) cells but not in older DIV26 cortical neurons.<sup>15</sup> At the time of the study,  $\beta$ -klotho was not believed to be expressed in cortical neurons at meaningful levels.<sup>18</sup> Thus, the ability of FGF21 to alter cell signaling pathways in young neurons was surprising. Moreover, its ineffectiveness on mature/older neuron cultures was further perplexing. Later, it was discovered that  $\beta$ -klotho is abundant in the human infant PFC but is comparatively absent in adults.<sup>9</sup> That discovery may in part explain the age-dependent discrepancy on neuronal FGF21 activity that was observed *in vitro*. That is, FGF21 may have preferentially altered RBM3 in young cortical neurons because  $\beta$ -klotho was transiently expressed at higher levels during immaturity. However, there was no evidence to support the key assumption that neurons are a major source of increased  $\beta$ -klotho in the developing brain. Here we confirm that  $\beta$ -klotho is indeed abundant in human

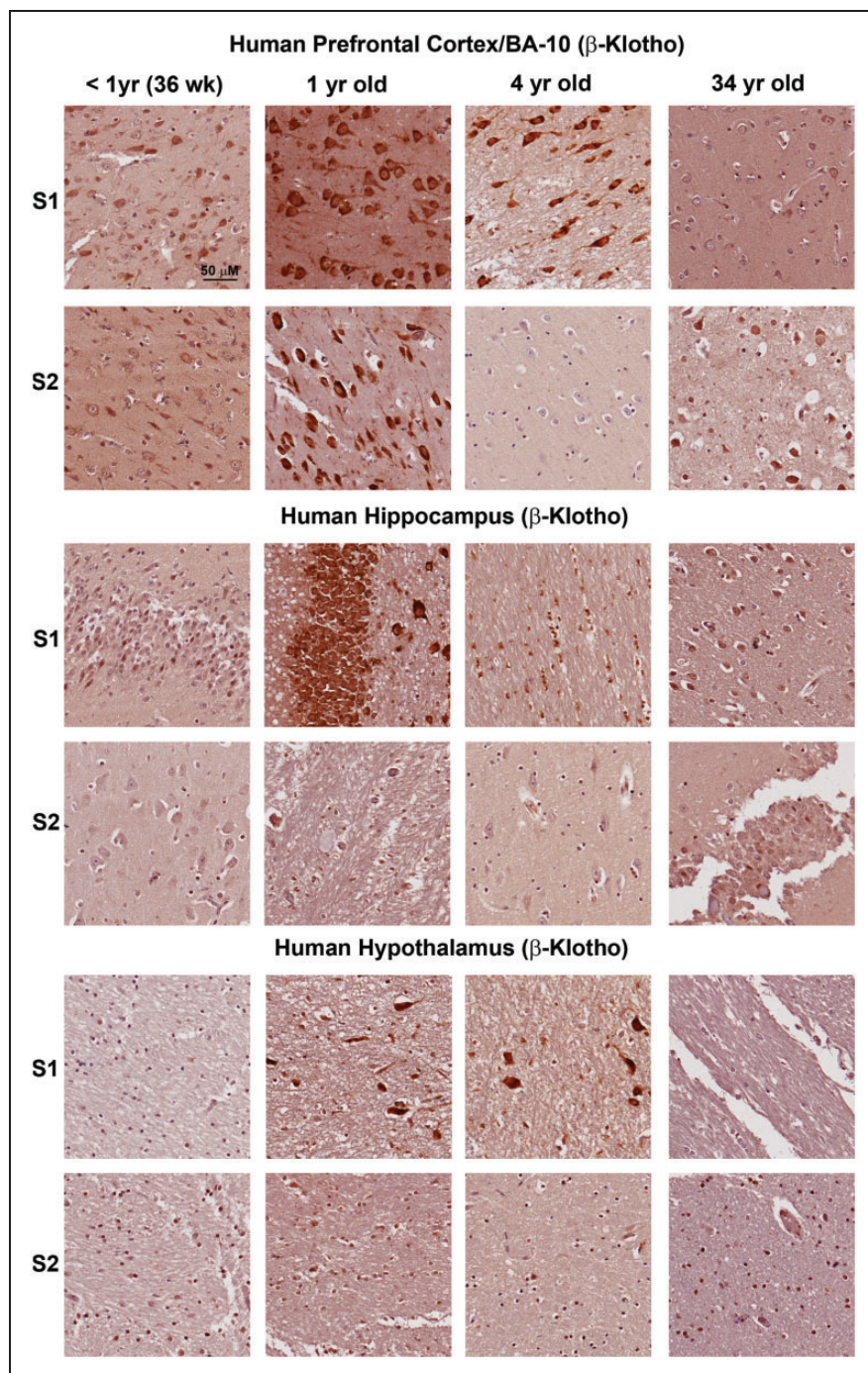


**Figure 5.** Comparison of  $\beta$ -klotho/hematoxylin counter staining across all ages (infant-to-adult). Images ( $10\times$  magnification) show representative staining levels of  $\beta$ -klotho (brown) for each age/brain region. Two different subjects within each age group are shown (S1 and S2). Relevant to the different brain regions,  $\beta$ -klotho staining intensity is greatest in the PFC > hippocampus > hypothalamus. Relevant to different ages, staining intensity in the hippocampus and cortex is greatest in 1 year-old vs. infants, 4 year-old, and 34 year-old). In infants, one year-olds, and four year-olds,  $\beta$ -klotho is visible in axonal projections from PFC neurons.

neurons in the young brain, as hypothesized. Staining in adult cortical tissues was comparatively decreased vs. younger subjects (mean  $\pm$  SD OD;  $8.65 \pm 0.70$  in adults vs.  $16.64 \pm 9.07$ ,  $85.01 \pm 56.71$ , and  $33.85 \pm 15.64$  in infants, 1 yr-olds, and 4 yr-olds, respectively). Thus,

we further hypothesize that  $\beta$ -klotho-regulated signaling pathways may be more robust and manipulatable in developing cortical neurons, whereas in adults FGF21 receptor activation in response to increased brain ligand disposition is either diminished or absent.



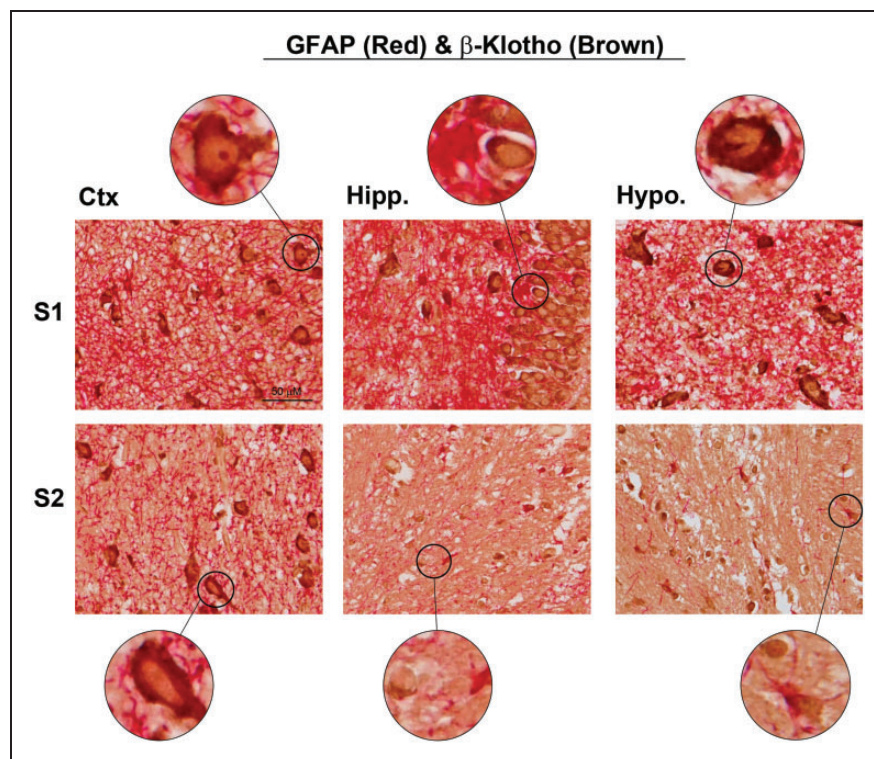


**Figure 6.**  $\beta$ -klotho and GFAP double-labeling in one-year-old tissue sections. Images ( $20\times$  magnification) show representative distribution of  $\beta$ -klotho (brown) and GFAP (red).  $\beta$ -klotho vs. GFAP staining does not co-localize. Circles show an enlarged view of typical cell staining patterns within each field.  $\beta$ -klotho (brown) intensity is greatest in the cell membrane/cytoplasm and is fainter in the nucleus.

More studies are needed to test that hypothesis, but our findings establish the clinical significance in addressing this question in future investigations.  $\beta$ -klotho staining was predominately membrane/cytoplasmic, which is consistent with (a) its function as a transmembrane co-receptor and (b) its pattern of distribution in over-expression studies in living cells.<sup>24</sup> Hypothalamic tissues were included for analysis because  $\beta$ -klotho expression is reportedly maintained into adulthood in that region, based on studies in mice.<sup>18</sup> Intriguingly, in human adults,  $\beta$ -klotho staining was increased in the human cortex/hippocampus vs. the hypothalamus (OD:  $8.56 \pm 0.70$  and  $7.27 \pm 1.07$  vs.  $3.37 \pm 2.45$ ). To our knowledge this is the first examination of  $\beta$ -klotho in the human brain, which may explain the discrepancy in our findings.

Exogenous FGF21 is neuroprotective in adult rodent models of brain injury (e.g. TBI and stroke). It is unclear if these effects are mediated by direct vs. indirect mechanisms.<sup>11,12</sup> Direct neuroprotective mechanisms involve the activation of FGF21 receptors on the surface of neurons which stimulate beneficial intracellular signaling changes. We showed that FGF21 augmented the levels of neuroprotective RBM3 in enriched DIV6-7 cortical neurons.<sup>15</sup> Leng et al. incubated DIV6

cortical neurons with FGF21 for six days and observed decreased cell death vs. vehicle controls after excitotoxic glutamate insult.<sup>25</sup> In addition, FGF21 application on DIV6 cortical neurons induced a temporary spike in the activation of the neuroprotective kinase phosphorylated protein kinase B (pAKT; peak levels were detected at 5 min post-treatment).<sup>25</sup> Given that  $\beta$ -klotho is essential for FGF21 ligand binding and it is increased in neurons at baseline in the immature brain, we speculate that direct neuroprotective effects mediated by systemic FGF21 release would therefore be more robust in young subjects. In contrast, in adults, indirect neuroprotective mechanisms (e.g. FGF21 stimulation of  $\beta$ -klotho expressing cells in the liver, adipose, and in the pancreas, which normalize glucose homeostasis and increase beneficial ketosis) may play a larger role in mediating CNS benefits, if they are observed.<sup>4</sup> In addition, FGF21 increased the expression of tight-junction proteins in endothelial cells which enhanced BBB integrity in a mouse model of type 2 diabetes.<sup>26</sup> FGF21 also decreased BBB damage in a model of TBI.<sup>12</sup> Additional studies in newborn rodents vs. adults are needed to disentangle the contributions of FGF21-induced neuroprotection that result from direct activation of receptors on the surface

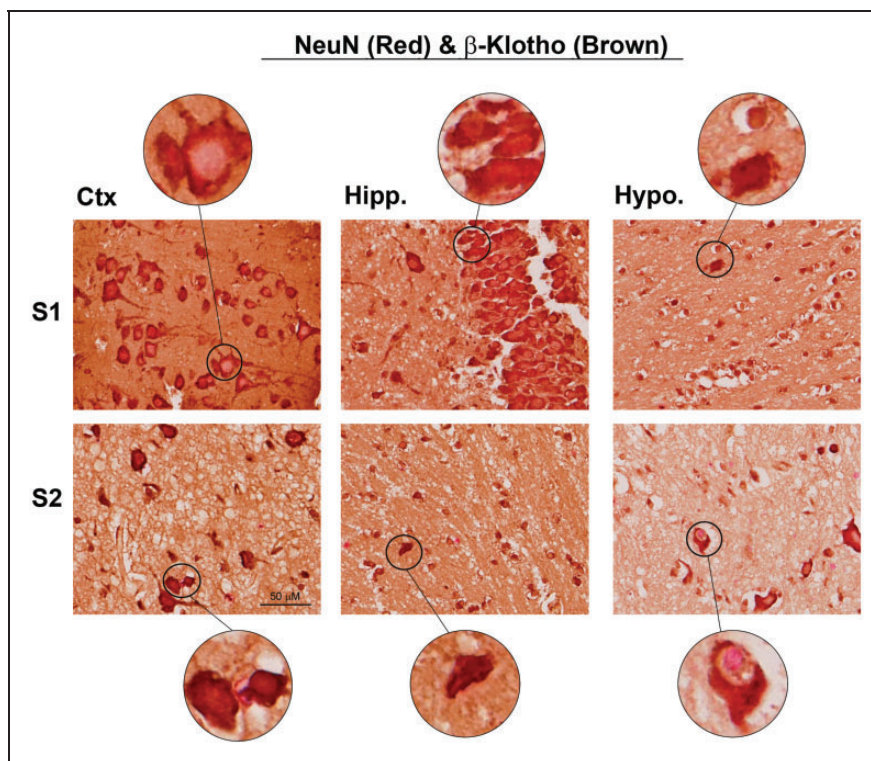


**Figure 7.**  $\beta$ -klotho and NeuN double-labeling in one-year-old tissue sections. Images ( $20\times$  magnification) show representative distribution of  $\beta$ -klotho (brown) and NeuN (red).  $\beta$ -klotho vs. NeuN staining results in a deep maroon color across all three brain regions, and is indicative of co-localization of brown/red labeling. Circles show an enlarged view of typical cell staining patterns within each field. In some neurons of the PFC and hypothalamus, the nuclear NeuN (red) can be distinguished from background due to decreased brown labeling in that particular subcellular compartment (i.e.  $\beta$ -klotho staining is lowest in the nucleus).

of neurons vs. benefits derived from non-neuronal origins. Furthermore, additional studies are needed to confirm that rodents have a comparable time course of neurodevelopmental  $\beta$ -klotho protein changes vs. humans.

Several limitations must be acknowledged. First, human brain tissue specimens were selected based on patient diagnosis (e.g. “unaffected controls”/NBB nomenclature). Thus, we avoided including patients who had chronic pathological brain diseases and/or other conditions that might confound interpretation of “baseline” RBM3 levels. Nevertheless, the way molecularly altering abnormal physiological states within our cohort may have influenced “baseline” RBM3 levels merits additional study. For instance, based on prior investigations in infants vs. adults, and on results here (Figure 1), we expected that  $<1$ -year-old infants would have the highest  $\beta$ -klotho staining in the hippocampus/PFC which was not seen. However,  $<1$ -year-old infants used for analysis here were born at 36 weeks, and thus it is unclear if the preterm brain may have different  $\beta$ -klotho expression vs. term newborns, or if it might have been altered by some aspect of pre-mortem care of preterm infants. Answers to these questions may have enormous clinical

importance and open up new avenues of research. Also, changes in body temperature, at the time of death and/or post-mortem, may have influenced RBM3 brain levels prior to tissue fixation. For instance, fever potentially decreases, whereas hypothermia increases, RBM3 expression.<sup>1,27</sup> Also, related to limitations in human tissues, we used a low number of replicates for each age group ( $n=2$ ). Nevertheless, the goal here was not to quantify the age-dependent change in brain RBM3/ $\beta$ -klotho expression, which has already been accomplished using appropriate techniques for addressing that specific biological question (e.g. Western blot). Rather, the primary goal here was to determine whether RBM3/ $\beta$ -klotho is expressed in injury-vulnerable neuronal populations in humans. Indeed, regardless of age group, RBM3/ $\beta$ -klotho demonstrated a clear preference in neurons across all patients.

Second, immunofluorescence is the preferred method to examine co-localization of multiple signals by IHC. As stated in the results, we explored immunofluorescent procedures on formalin-fixed paraffin embedded (FFPE) brain tissues but had little success due to confounding background auto-fluorescence. Difficulties overcoming background fluorescence were compounded using monoclonal cell-type specific antibodies.

Monoclonal antibodies are highly specific but often have lower signal amplification post-secondary because they detect a single antigenic epitope vs. polyclonals. The issue of auto-fluorescence is a well-recognized problem.<sup>28</sup> In fact, fixation-induced auto-fluorescence has been exploited to image the brain microarchitecture.<sup>29</sup> Alternatively, chromogenic approaches have been successfully used to counter-stain multiple proteins in human tissue sections, and readily distinguish numerous targets if they have little overlap.<sup>30,31</sup> Using the latter approach, we found that RBM3/ $\beta$ -klotho had strong overlap with NeuN but not with GFAP. Importantly, to strengthen the underpinnings of these studies, we confirmed the specificity of RBM3/ $\beta$ -klotho antibodies. Both polyclonal antibodies (a) detected a single band (at the anticipated molecular weight; Figure 1) in human brain tissue homogenates, which were from the brain regions of interest also analyzed by IHC, (b) showed the expected differences in age-dependent expression, and (c) were previously validated.<sup>9</sup> More studies are needed to screen/identify alternative high-quality monoclonal antibodies for additional cell-type markers to detect microglia, oligodendrocytes, or brain endothelial cells, and to determine their potential co-localization with RBM3/ $\beta$ -klotho. However, immunofluorescent studies in rodents showed that RBM3 mainly co-localized with neurons and had minimal overlap with 2',3'-cyclic-nucleotide 3'-phosphodiesterase or GFAP in the cortex, hippocampus, or cerebellum.<sup>8</sup> Germane to the primary goal of this study, we think that the results convincingly demonstrate that RBM3 and  $\beta$ -klotho are abundant in neurons in the developing brain. We speculate that both proteins are expressed at lower levels in non-neuronal CNS cells in humans, and perhaps in other brain regions at older ages. Additional work is needed to test that hypothesis by IHC. It may also be possible to separate neurons vs. glia-types in the CNS using fluorescence-activated cell sorting on fresh or frozen human brain tissues, for a quantitative comparison of RBM3/ $\beta$ -klotho levels across cell types.<sup>32</sup>

Finally, there were additional limitations related to specimen selection. First, rectangular (cm sized) pieces of fixed brain tissues were generously provided by the NIH NBB. Specimens from brain loci (e.g. hippocampus, cortex, or hypothalamus) appeared heterogeneous in composition (e.g. differences in white vs. grey matter content and/or in the x/y/z plane for each anatomical slice). For instance, the stratum pyramidale was visible in some hippocampal specimens but not in others, suggesting that tissues were from different hippocampal subfields. Furthermore, preparation of slides for paraffin embedding required that a smaller (mm sized) area of tissue be isolated from within each specimen for mounting (i.e. to fit all 24 representative specimens on a single glass slide and equalize IHC treatments across

samples; Figures 2 and 5). To protocolize sampling, we used an 8-mm biopsy puncher to pick equivalent-sized round tissues at the center of each specimen. However, this approach, although maximizing rigor and limiting sampling bias, likely produced an unavoidable increase in staining variability across specimens, with some specimens having more white matter with fewer neurons. However, because our goal was to investigate the signal distribution among CNS cells within individual specimens, rather than to quantify levels across samples, we think individual sample selection bias was a minor concern; moreover, the fact that white matter enriched sections had much lower RBM3/ $\beta$ -klotho staining further supports the conclusion that these targets are enriched in neurons. Second, it would have been ideal to link the IHC staining in fixed human brain to the same subjects previously used to measure RBM3/ $\beta$ -klotho levels in whole brain tissue homogenates. This was not feasible due to limitations in sample availability. Thus, most fixed-brain tissue specimens in these follow-up IHC investigations were different subjects vs. those used in prior Western blot studies (except for subjects #4428, #451, and #5648). Finally, prior analysis of data collapsed by age did not reveal gender-specific differences in human brain RBM3 and  $\beta$ -klotho protein levels.<sup>9</sup> Thus, to minimize redundancy in the use of precious NBB specimens, we limited IHC analysis to male subjects. Nevertheless, we cannot rule out the possibility that a much larger sample size would reveal effects of gender on the localization and/or levels of RBM3/ $\beta$ -klotho in specific cell-types. Additional studies are needed to address that limitation.

In conclusion, here we build upon prior studies which showed that RBM3/ $\beta$ -klotho is increased in the immature brain vs. adults. Specifically, this study adds to that body of work by showing that neurons are a major source of increased RBM3/ $\beta$ -klotho levels in the developing brain. Moreover, the results suggest that cold-shock/stress signaling mechanisms are critical for neurons during CNS maturation. However, the downstream mechanisms affected by the temporal upregulation of these pathways remain to be elucidated. Finally, IHC data from the adult brain add to the growing body of evidence which suggests that cold-shock/stress signaling mechanisms in the CNS are decreased in older populations. We speculate that novel strategies to upregulate RBM3/ $\beta$ -klotho in neurons, independent of age, are an important therapeutic objective in the setting of brain injury and merit further exploration.

## Funding

The author(s) disclosed receipt of the following financial support for the research, authorship, and/or publication of this article: NIH/NINDS grants R21NS098057 and R01NS105721 to TCJ, by the Ake N Grenvik Chair in

Critical Care Medicine (PMK), and by University of South Florida Morsani College of Medicine start-up funds to TCJ.

### Acknowledgements

We are grateful to the NIH NeuroBioBank for providing human tissues used in this study. Tissues were made available upon completion and acceptance of a signed Material Transfer Agreement between the University of Pittsburgh and the NBB.

### Declaration of conflicting interests

The author(s) declared the following potential conflicts of interest with respect to the research, authorship, and/or publication of this article: Travis C Jackson and Patrick M Kochanek are co-inventors on a pending patent on the use of FGF21 therapy in temperature managed patients and titled: "Method to Improve Neurologic Outcomes in Temperature Managed Patients" (USPTO Application No. 15/573,006).

### Authors' contributions

TCJ designed the study. TCJ, KJF, SWC, and SEK performed experiments. TCJ, PMK, SWC, and KJF contributed to data analysis and interpretation. TCJ and PMK wrote the manuscript.

### Supplemental material

Supplemental material for this paper can be found at the journal website: <http://journals.sagepub.com/home/jcb>

### References

1. Chip S, Zelmer A, Ogunshola OO, et al. The RNA-binding protein RBM3 is involved in hypothermia induced neuroprotection. *Neurobiol Dis* 2011; 43: 388–396.
2. Peretti D, Bastide A, Radford H, et al. RBM3 mediates structural plasticity and protective effects of cooling in neurodegeneration. *Nature* 2015; 518: 236–239.
3. Bastide A, Peretti D, Knight JR, et al. RTN3 is a novel cold-induced protein and mediates neuroprotective effects of RBM3. *Curr Biol* 2017; 27: 638–650.
4. Jackson TC and Kochanek PM. A new vision for therapeutic hypothermia in the era of targeted temperature management: a speculative synthesis. *Ther Hypothermia Temp Manage* 2019; 9.
5. Dresios J, Aschrafi A, Owens GC, et al. Cold stress-induced protein Rbm3 binds 60S ribosomal subunits, alters microRNA levels, and enhances global protein synthesis. *Proc Natl Acad Sci U S A* 2005; 102: 1865–1870.
6. Smart F, Aschrafi A, Atkins A, et al. Two isoforms of the cold-inducible mRNA-binding protein RBM3 localize to dendrites and promote translation. *J Neurochem* 2007; 101: 1367–1379.
7. Pilotte J, Dupont-Versteegden EE and Vanderklish PW. Widespread regulation of miRNA biogenesis at the Dicer step by the cold-inducible RNA-binding protein, RBM3. *PLoS One* 2011; 6: e28446.
8. Pilotte J, Cunningham BA, Edelman GM, et al. Developmentally regulated expression of the cold-inducible RNA-binding motif protein 3 in euthermic rat brain. *Brain Res* 2009; 1258: 12–24.
9. Jackson TC, Kotermanski SE and Kochanek PM. Infants uniquely express high levels of RBM3 and other cold-adaptive neuroprotectant proteins in the human brain. *Dev Neurosci* 2018; 40: 325–336.
10. Hsueh H, Pan W and Kastin AJ. The fasting polypeptide FGF21 can enter brain from blood. *Peptides* 2007; 28: 2382–2386.
11. Jiang Y, Liu N, Wang Q, et al. Endocrine regulator rFGF21 (recombinant human fibroblast growth factor 21) improves neurological outcomes following focal ischemic stroke of type 2 diabetes mellitus male mice. *Stroke* 2018; 49: 3039–3049.
12. Chen J, Hu J, Liu H, et al. FGF21 protects the blood-brain barrier by upregulating PPARgamma via FGFR1/beta-klotho after traumatic brain injury. *J Neurotrauma* 2018; 35: 2091–2103.
13. Ameka M, Markan KR, Morgan DA, et al. Liver derived FGF21 maintains core body temperature during acute cold exposure. *Sci Rep* 2019; 9: 630.
14. Lee P, Brychta RJ, Linderman J, et al. Mild cold exposure modulates fibroblast growth factor 21 (FGF21) diurnal rhythm in humans: relationship between FGF21 levels, lipolysis, and cold-induced thermogenesis. *J Clin Endocrinol Metab* 2013; 98: E98–102.
15. Jackson TC, Manole MD, Kotermanski SE, et al. Cold stress protein RBM3 responds to temperature change in an ultra-sensitive manner in young neurons. *Neuroscience* 2015; 305: 268–278.
16. Ogawa Y, Kurosu H, Yamamoto M, et al. beta Klotho is required for metabolic activity of fibroblast growth factor 21. *Proc Natl Acad Sci U S A* 2007; 104: 7432–7437.
17. Adams AC, Cheng CC, Coskun T, et al. FGF21 requires beta klotho to act in vivo. *Plos One* 2012; 7.
18. Bookout AL, de Groot MHM, Owen BM, et al. FGF21 regulates metabolism and circadian behavior by acting on the nervous system. *Nat Med* 2013; 19: 1147–1152.
19. Talukdar S, Owen BM, Song P, et al. FGF21 regulates sweet and alcohol preference. *Cell Metab* 2016; 23: 344–349.
20. Jackson TC, Dixon CE, Janesko-Feldman K, et al. Acute physiology and neurologic outcomes after brain injury in SCOP/PHLPP1 KO mice. *Sci Rep* 2018; 8: 7158.
21. Zhang HT, Zhang ZW, Xue JH, et al. Differential expression of the RNA-binding motif protein 3 in human astrocytoma. *Chin Med J* 2013; 126: 1948–1952.
22. Papadima EM, Niola P, Melis C, et al. Evidence towards RNA binding motif (RNP1, RRM) protein 3 (RBM3) as a potential biomarker of lithium response in bipolar disorder patients. *J Mol Neurosci* 2017; 62: 304–308.
23. von Holstein-Rathlou S, BonDurant LD, Peltekian L, et al. FGF21 mediates endocrine control of simple sugar intake and sweet taste preference by the liver. *Cell Metab* 2016; 23: 335–343.
24. Ming AYC, Yoo E, Vorontsov EN, et al. Dynamics and distribution of klotho beta (KLB) and fibroblast growth factor receptor-1 (FGFR1) in living cells reveal the

- fibroblast growth factor-21 (FGF21)-induced receptor complex. *J Biol Chem* 2012; 287: 19997–20006.
25. Leng Y, Wang Z, Tsai LK, et al. FGF-21, a novel metabolic regulator, has a robust neuroprotective role and is markedly elevated in neurons by mood stabilizers. *Mol Psychiatry* 2015; 20: 215–223.
  26. Yu ZY, Lin L, Jiang YH, et al. Recombinant FGF21 protects against blood-brain barrier leakage through Nrf2 upregulation in type 2 diabetes mice. *Mol Neurobiol* 2019; 56: 2314–2327.
  27. Wong JLL, Au AYM, Gao DD, et al. RBM3 regulates temperature sensitive miR-142-5p and miR-143 (thermomirs), which target immune genes and control fever. *Nucleic Acids Res* 2016; 44: 2888–2897.
  28. Kajimura J, Ito R, Manley NR, et al. Optimization of single- and dual-color immunofluorescence protocols for formalin-fixed, paraffin-embedded archival tissues. *J Histochem Cytochem* 2016; 64: 112–124.
  29. Leischner U, Schierloh A, Zieglansberger W, et al. Formalin-induced fluorescence reveals cell shape and morphology in biological tissue samples. *PLoS One* 2010; 5: e10391.
  30. Tumei PC, Harview CL, Yearley JH, et al. PD-1 blockade induces responses by inhibiting adaptive immune resistance. *Nature* 2014; 515: 568–571.
  31. Ilie M, Beaulande M, Ben Hadj S, et al. Chromogenic multiplex immunohistochemistry reveals modulation of the immune microenvironment associated with survival in elderly patients with lung adenocarcinoma. *Cancers* 2018; 10.
  32. Rubio FJ, Li X, Liu QR, et al. Fluorescence activated cell sorting (FACS) and gene expression analysis of Fos-expressing neurons from fresh and frozen rat brain tissue. *J Vis Exp* 2016; (114): 54358.